Chemi-ionization/recombination Atomic Processes in the AGNs Broad-Line Region

Vladimir A. SREĆKOVIĆ[1], Milan S. DIMITRIJEVIĆ[2], Ljubinko M. IGNJATOVIĆ[1]

[1]Institute of Physics, P.O.Box 57, Pregrevica 118, Belgrade, Serbia

[2]Astronomical Observatory, Volgina 7, 11060 Belgrade, Serbia

vlada@ipb.ac.rs

Thank you for your attention

• Sreckovic Vladimir vlada@ipb.ac.rs

Institute of Physics Belgrade, University of Belgrade, Serbia

Serbia's First National Institute

<u>research interest</u>: Solar and stellar astrophysics; High energy astrophysics; Atomic and ionic collisions with formation of quasimolecules; Atomic processes in white dwarfs and solar type stars; Astroinformatics; Databases; Space Weather studies of Upper Atmosphere; Ionospheric plasma Irregularities using VLF .

Also, people from the IF team (in this field of joint research): Lj. Ignjatovic …

AOB team i.e. collaborators in this thematic: M. Dimitrijević, and others

Astronomical Observatory, Belgrade, Serbia

IF: very nice place

this topic: We *collaborate with* prof. A. N. Klyucharev and Bezuglov, Nikolai Department of Physics, Saint-Petersburg University, Ulianovskaya 1, Petrodvorets, St. Petersburg, Russia 198504

ELSEVIER

CrossMark

Available online at www.sciencedirect.com

ScienceDirect

Advances in Space Research 54 (2014) 1159–1163

ADVANCES IN SPACE RESEARCH (a COSPAR publication)

www.elsevier.com/locate/asr

Anomalies in radiation-collisional kinetics of Rydberg atoms induced by the effects of dynamical chaos and the double Stark resonance

N.N. Bezuglov [a,c], A.N. Klyucharev [a], A.A. Mihajlov [b], V.A. Srećković [b,*]

[a] Department of Physics, Saint-Petersburg University, Ulianovskaya 1, 198504, Petrodvorets, St. Petersburg, Russia
[b] University of Belgrade, Institute of Physics, P.O. Box 57, 11001 Belgrade, Serbia
[c] Laser Centre, University of Latvia, Zellu Str. 8, LV-1002 Riga, Latvia

J Clust Sci (2012) 23:47–75
DOI 10.1007/s10876-011-0438-7

REVIEW PAPER

The Chemi-Ionization Processes in Slow Collisions of Rydberg Atoms with Ground State Atoms: Mechanism and Applications

A. A. Mihajlov · V. A. Srećković · Lj. M. Ignjatović · A. N. Klyucharev

Chemi-ionization/recombination processes in solar photosphere

INTRO: Solar photosphere and M Red Dwarfs before AGN BLR topic

Few years ago we started investigations of chemi-ionization/recombination processes and their influence in solar photosphere

The Astrophysical Journal Supplement Series, 193:2 (7pp), 2011 March
doi:10.1088/0067-0049/193/1/2
© 2011. The American Astronomical Society. All rights reserved. Printed in the U.S.A.

CHEMI-IONIZATION IN SOLAR PHOTOSPHERE: INFLUENCE ON THE HYDROGEN ATOM EXCITED STATES POPULATION

Anatolij A. Mihajlov[1,2], Ljubinko M. Ignjatović[1,2], Vladimir A. Srećković[1], and Milan S. Dimitrijević[2,3,4]
[1] Institute of Physics, University of Belgrade, P.O. Box 57, 11001 Belgrade, Serbia; ljuba@ipb.ac.rs, mihajlov@ipb.ac.rs
[2] Isaac Newton Institute of Chile, Yugoslavia Branch, Volgina 7, 11060 Belgrade, Serbia
[3] Astronomical Observatory, Volgina 7, 11060 Belgrade, Serbia
[4] Observatoire de Paris, 92195 Meudon Cedex, France
Received 2010 May 30; accepted 2010 December 5; published 2011 January 18

ABSTRACT

In this paper, the influence of chemi-ionization processes in $H^*(n \geqslant 2) + H(1s)$ collisions, as well as the influence of inverse chemi-recombination processes on hydrogen atom excited-state populations in solar photosphere, are compared with the influence of concurrent electron–atom and electron–ion ionization and recombination processes. It has been found that the considered chemi-ionization/recombination processes dominate over the relevant concurrent processes in almost the whole solar photosphere. Thus, it is shown that these processes and their importance for the non-local thermodynamic equilibrium modeling of the solar atmosphere should be investigated further.

In Mihajlov et al. 2011 we investigated chemi-ionization/recombination processes in H*(n) + H(1s) collisions and their influence on the populations of hydrogen Rydberg atoms and electrons in weakly ionized layers of the Solar photosphere and the lower chromosphere

chemi-ionization processes:

$$H^*(n) + H(1s) \Rightarrow H_2^+ + e,$$ Associative chemi-ionization channel i.e. creation of H_2^+

$$H^*(n) + H(1s) \Rightarrow H(1s) + H^+ + e,$$ Non-associative ionization ch.

Invers chemi-recombination processes:

$$H_2^+ + e \Rightarrow H^*(n) + H(1s),$$

$$H(1s) + H^+ + e \Rightarrow H^*(n) + H(1s),$$

We compare with the corresponding electron-atom collision processes

$$H^*(n) + e \Rightarrow H^+ + 2e,$$

$$H^+ + 2e \Rightarrow H^*(n) + e,$$

$$H^+ + e \Rightarrow H^*(n) + \varepsilon_\lambda,$$

Mechanism is described in details in review paper Mihajlov et al. 2012

$A^*(n) + A$ is represented as $[A^+ + {}^*A(1s)] + e$
system of quasi molecule and electron

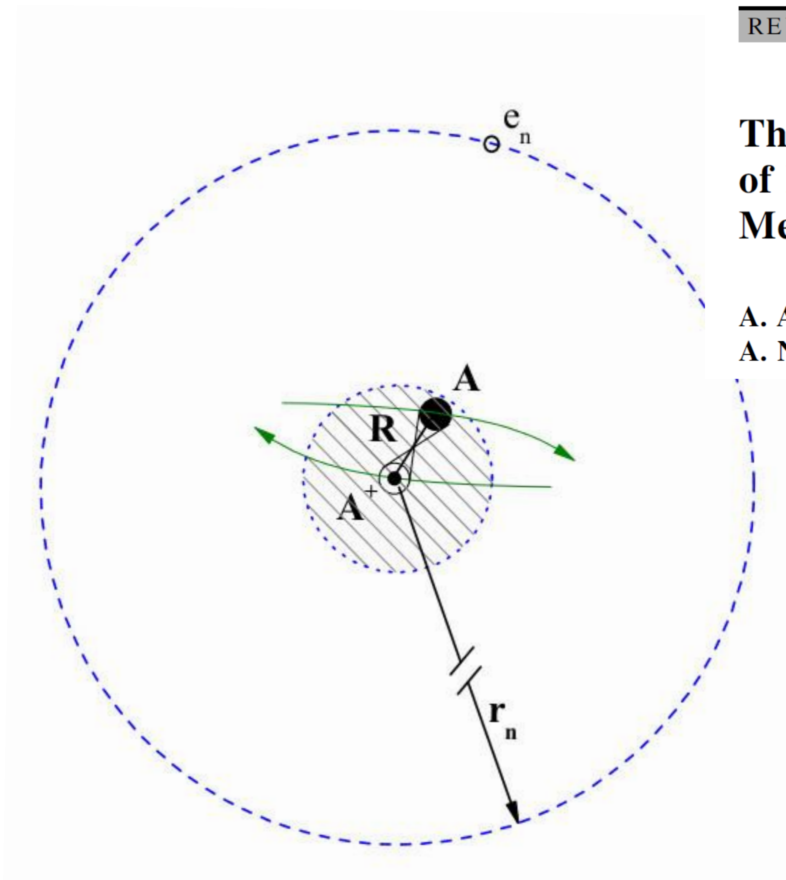

J Clust Sci (2012) 23:47–75
DOI 10.1007/s10876-011-0438-7

REVIEW PAPER

The Chemi-Ionization Processes in Slow Collisions of Rydberg Atoms with Ground State Atoms: Mechanism and Applications

A. A. Mihajlov · V. A. Srećković · Lj. M. Ignjatović · A. N. Klyucharev

[illegible]

[illegible]

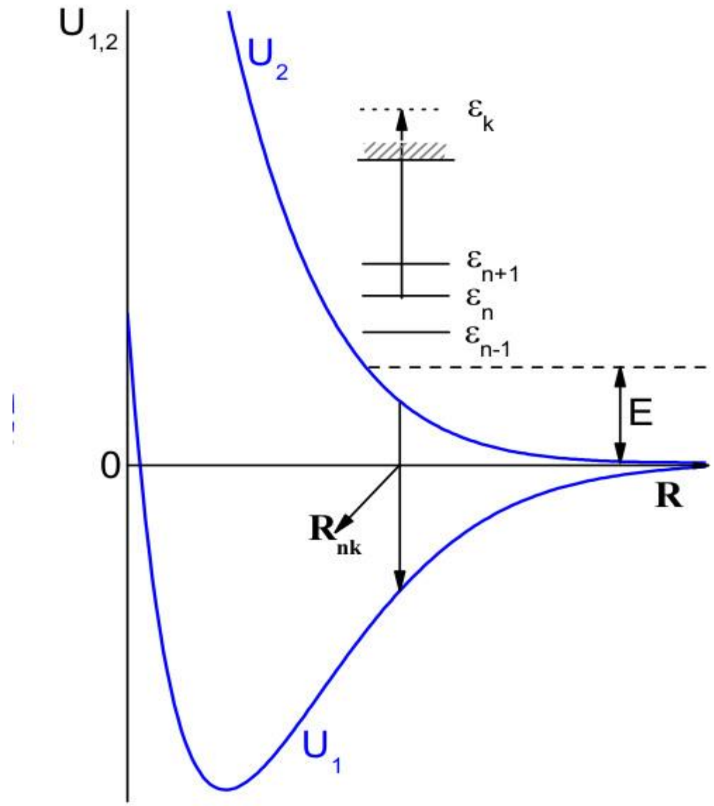

(b)

First we calculate cross sections and rate coefficients for the conditions that exists in weakly ionized layers of the Solar photosphere and the lower chromosphere.

These data are input parameters needed for modeling.

$$H^*(n) + H(1s) \Rightarrow H_2^+ + e, \quad \text{a)}$$

$$H^*(n) + H(1s) \Rightarrow H(1s) + H^+ + e, \quad \text{b)}$$

Cross sections for channel a) and b)

$$\sigma_{ci}^{(a,b)}(n, E) = 2\pi \int_0^{\rho_{max}^{(a,b)}(E)} P_{ci}^{(a,b)}(n, \rho, E)\rho d\rho,$$

Rate coefficient for channel a) and b)

$$K_{ci}^{(a,b)}(n, T) = \int_{E_{min}^{(a,b)}(n)}^{E_{max}} v\sigma_{ci}^{(a,b)}(n, E) f(v; T) dv,$$

Total rate coefficient

$$K_{ci}(n, T) = K_{ci}^{(a)}(n, T) + K_{ci}^{(b)}(n, T),$$

Table 1
Calculated Values of Coefficient K_{ci} ($cm^3\ s^{-1}$) as a Function of n and T

T (K)	n						
	2	3	4	5	6	7	8
4000	0.150E−11	0.619E−09	0.126E−08	0.576E−09	0.554E−09	0.463E−09	0.366E−09
4250	0.202E−11	0.549E−09	0.106E−08	0.617E−09	0.583E−09	0.482E−09	0.378E−09
4500	0.260E−11	0.501E−09	0.900E−09	0.656E−09	0.611E−09	0.500E−09	0.389E−09
4750	0.324E−11	0.488E−09	0.833E−09	0.694E−09	0.637E−09	0.517E−09	0.400E−09
5000	0.403E−11	0.495E−09	0.815E−09	0.730E−09	0.662E−09	0.533E−09	0.410E−09
5250	0.504E−11	0.501E−09	0.800E−09	0.765E−09	0.686E−09	0.548E−09	0.420E−09
5500	0.623E−11	0.500E−09	0.782E−09	0.799E−09	0.709E−09	0.563E−09	0.428E−09
5750	0.756E−11	0.493E−09	0.764E−09	0.832E−09	0.731E−09	0.576E−09	0.437E−09
6000	0.909E−11	0.490E−09	0.757E−09	0.864E−09	0.752E−09	0.589E−09	0.445E−09
6250	0.108E−10	0.502E−09	0.766E−09	0.895E−09	0.772E−09	0.602E−09	0.453E−09
6500	0.128E−10	0.519E−09	0.783E−09	0.924E−09	0.791E−09	0.613E−09	0.460E−09
7000	0.175E−10	0.540E−09	0.808E−09	0.981E−09	0.827E−09	0.635E−09	0.473E−09
7500	0.232E−10	0.574E−09	0.848E−09	0.103E−08	0.860E−09	0.655E−09	0.485E−09
8000	0.300E−10	0.609E−09	0.891E−09	0.108E−08	0.892E−09	0.674E−09	0.497E−09
8500	0.380E−10	0.650E−09	0.939E−09	0.113E−08	0.920E−09	0.691E−09	0.507E−09
9000	0.470E−10	0.688E−09	0.986E−09	0.118E−08	0.948E−09	0.707E−09	0.516E−09
9500	0.574E−10	0.733E−09	0.104E−08	0.122E−08	0.973E−09	0.722E−09	0.525E−09
10000	0.689E−10	0.787E−09	0.109E−08	0.126E−08	0.997E−09	0.736E−09	0.533E−09

Table 2

Calculated Values of Recombination Coefficient K_{cr} ($cm^6\ s^{-1}$) as a Function of n and T

T (K)	n						
	2	3	4	5	6	7	8
4000	0.190E−27	0.732E−27	0.390E−27	0.114E−27	0.977E−28	0.831E−28	0.709E−28
4250	0.130E−27	0.458E−27	0.257E−27	0.102E−27	0.880E−28	0.753E−28	0.645E−28
4500	0.918E−28	0.305E−27	0.177E−27	0.914E−28	0.799E−28	0.688E−28	0.591E−28
4750	0.666E−28	0.223E−27	0.135E−27	0.828E−28	0.730E−28	0.631E−28	0.544E−28
5000	0.506E−28	0.174E−27	0.110E−27	0.755E−28	0.671E−28	0.582E−28	0.503E−28
5250	0.403E−28	0.138E−27	0.912E−28	0.693E−28	0.619E−28	0.540E−28	0.467E−28
5500	0.331E−28	0.111E−27	0.763E−28	0.639E−28	0.575E−28	0.502E−28	0.436E−28
5750	0.275E−28	0.889E−28	0.645E−28	0.592E−28	0.535E−28	0.469E−28	0.407E−28
6000	0.233E−28	0.731E−28	0.558E−28	0.551E−28	0.500E−28	0.440E−28	0.382E−28
6250	0.201E−28	0.627E−28	0.498E−28	0.514E−28	0.469E−28	0.413E−28	0.360E−28
6500	0.176E−28	0.548E−28	0.451E−28	0.482E−28	0.441E−28	0.389E−28	0.339E−28
7000	0.139E−28	0.421E−28	0.374E−28	0.427E−28	0.393E−28	0.348E−28	0.304E−28
7500	0.114E−28	0.341E−28	0.322E−28	0.382E−28	0.354E−28	0.314E−28	0.275E−28
8000	0.964E−29	0.284E−28	0.283E−28	0.345E−28	0.321E−28	0.286E−28	0.250E−28
8500	0.834E−29	0.243E−28	0.253E−28	0.314E−28	0.293E−28	0.261E−28	0.229E−28
9000	0.731E−29	0.211E−28	0.229E−28	0.287E−28	0.269E−28	0.240E−28	0.211E−28
9500	0.654E−29	0.187E−28	0.209E−28	0.264E−28	0.248E−28	0.222E−28	0.195E−28
10000	0.590E−29	0.169E−28	0.194E−28	0.245E−28	0.230E−28	0.206E−28	0.181E−28

the <u>first conclusion</u> in the paper Mihajlov et al. 2011 relates to relative contribution of partial chemi-ionization and recombination processes i.e. channels a) and b) for given *n* and *T*

Table 3
Calculated Values of Coefficient $X^{(a)} \equiv K_{\rm ci}^{(a)}/K_{\rm ci} = K_{\rm cr}^{(a)}/K_{\rm cr}$ as a Function of n and T

T (K)	n						
	2	3	4	5	6	7	8
4000	0.998	0.955	0.877	0.507	0.408	0.335	0.281
4250	0.969	0.934	0.827	0.484	0.388	0.318	0.266
4500	0.924	0.907	0.765	0.463	0.371	0.303	0.254
4750	0.872	0.881	0.709	0.443	0.354	0.289	0.242
5000	0.819	0.857	0.664	0.425	0.339	0.277	0.231
5250	0.769	0.831	0.619	0.408	0.325	0.265	0.221
5500	0.721	0.800	0.568	0.393	0.312	0.254	0.212
5750	0.673	0.764	0.515	0.378	0.300	0.244	0.203
6000	0.627	0.728	0.466	0.364	0.288	0.235	0.196
6250	0.585	0.699	0.430	0.351	0.278	0.226	0.188
6500	0.546	0.672	0.399	0.339	0.268	0.218	0.182
7000	0.474	0.610	0.336	0.317	0.250	0.204	0.169
7500	0.414	0.558	0.289	0.297	0.235	0.190	0.158
8000	0.363	0.510	0.250	0.280	0.221	0.179	0.149
8500	0.321	0.469	0.220	0.264	0.208	0.169	0.141
9000	0.287	0.429	0.193	0.250	0.197	0.160	0.133
9500	0.258	0.398	0.174	0.237	0.187	0.151	0.126
10000	0.234	0.376	0.160	0.225	0.177	0.144	0.120

$$H^*(n) + H(1s) \Rightarrow H_2^+ + e, \quad \text{(a)}$$

$$H^*(n) + H(1s) \Rightarrow H(1s) + H^+ + e, \quad \text{(b)}$$

branch coefficients ratio

$$X_{\rm ci}^{(a,b)}(n,T) = \frac{K_{\rm ci}^{(a,b)}(n,T)}{K_{\rm ci}(n,T)},$$

second conclusion relates to the comparison with the corresponding electron-atom collision processes

Comparison of Fluxes of the Considered Proces

$$I_{ci}(n,T) = K_{ci}(n,T) \cdot N_n N_1,$$
$$I_{cr}(n,T) = K_{cr}(n,T) \cdot N_1 N_i N_e,$$

$$I_{i;ea}(n,T) = K_{ea}(n,T) \cdot N_n N_e,$$
$$I_{r;eei}(n,T) = K_{eei}(n,T) \cdot N_i N_e N_e,$$
$$I_{r;ph}(n,T) = K_{ph}(n,T) \cdot N_i N_e,$$

$$F_i(n,T) = \frac{I_{ci}(n,T)}{I_{i;ea}(n,T)} = \frac{K_{ci}(n,T)}{K_{ea}(n,T)} \cdot N_1 N_e,$$

$$F_{i,ea;2-8}(T) = \frac{\sum_{n=2}^{8} I_{ci}(n,T)}{\sum_{n=2}^{8} I_{i;ea}(n,T)}$$

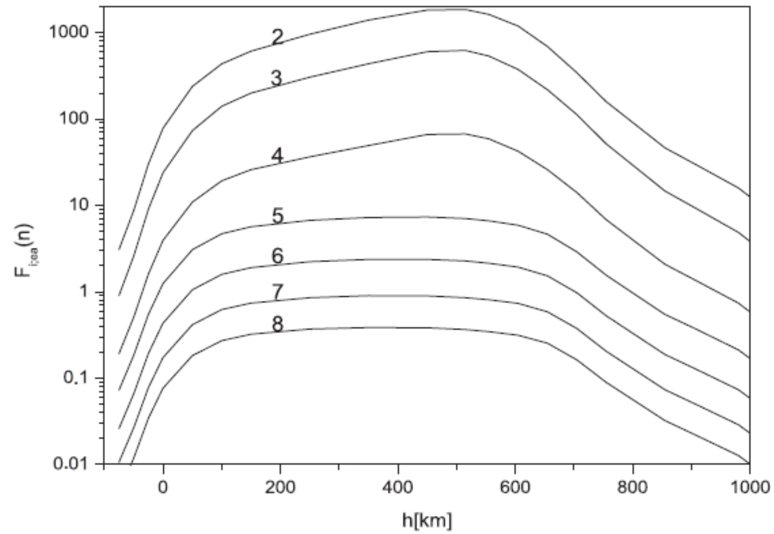

It has been demonstrated in Mihajlov et al. (2011) that Chemi-ionization/recombination processes in H(n) + H(1s) collisions, for the principal quantum number n>2, must have significant influence in comparison with the corresponding electron-atom collision processes on the populations of hydrogen Rydberg atoms and electrons in weakly ionized layers of the Solar photosphere and the lower chromosphere, and that they have to be included in modelling and investigation of Solar plasma, especially in the region of the temperature minimum in the Solar photosphere.

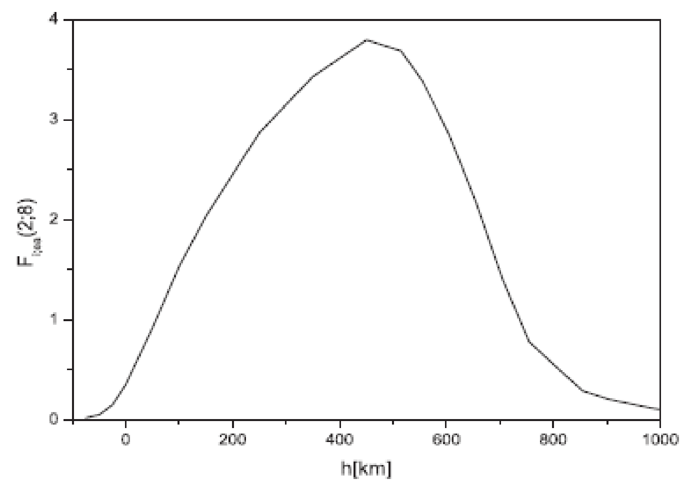

Figure 4. Behavior of the quantity $F_{i;ea}(2;8)$ given by Equation (29), as a function of height h.

ELSEVIER
Contents lists available at ScienceDirect
New Astronomy Reviews
journal homepage: www.elsevier.com/locate/newastrev

Rydberg atoms in astrophysics

Yu.N. Gnedin [a], A.A. Mihajlov [b], Lj.M. Ignjatović [b], N.M. Sakan [b], V.A. Srećković [b,*], M.Yu. Zakharov [c], N.N. Bezuglov [c], A.N. Klycharev [c]

[a] Central Astronomical Observatory, Pulkovo, RAS, Russia
[b] Institute of Physics, P.O. Box 57, 11001 Belgrade, Serbia
[c] Department of Physics, Saint-Petersburg University, Ulianovskaya 1, 198504 St. Petersburg, Petrodvorets, Russia

The presented results suggest that the chemi-ionization/recombination processes due to their influence on the excited state populations and the free electron density, also should influence on the atomic spectral line shapes.

This assumption is confirmed by the Figs, which show the profiles of some of hydrogen spectral lines in the M red stars calculated with and without these processes using PHOENIX code.

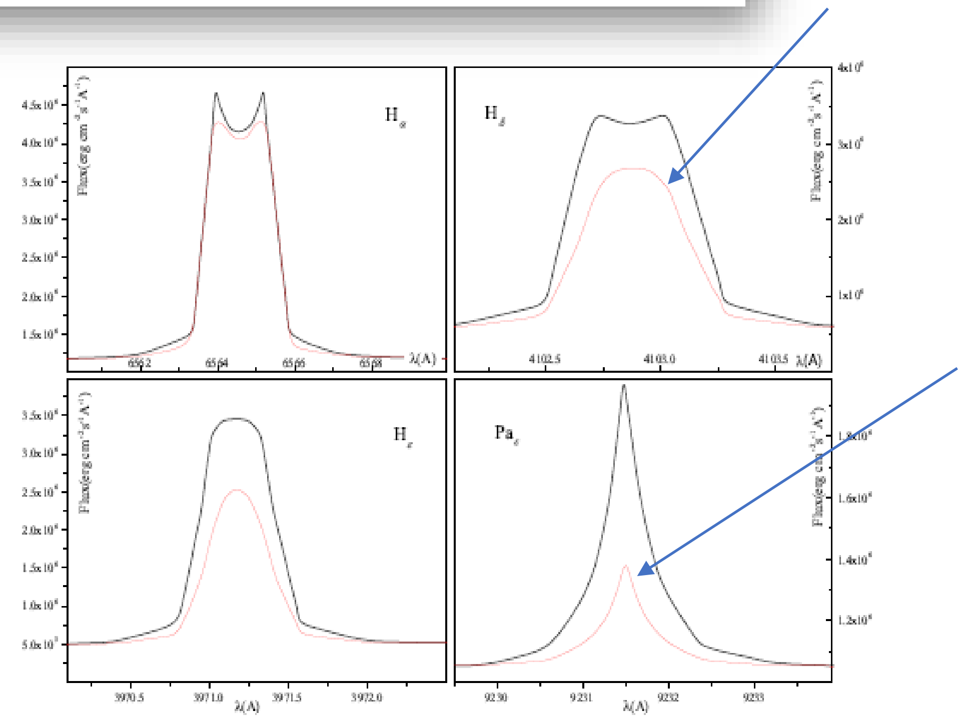

Figure 13. Line profiles with (full) and without (red tiny) inclusion of chemi-ionization and chemi-recombination processes for H lines.

Figure 13 (from [26]) show the line profiles of H_α, H_δ, H_ε Pa_ε with and without inclusion of processes (1). Profiles are synthesized with PHOENIX code with Stark broadening contribution calculated using tables from [40] for Stark broadening of hydrogen lines (linear Stark effect). Lineshape changes, especially in the wings, show the influence of the electron density change having a direct influence on the Stark broadening of hydrogen lines.

Let's go back to the Chemi-ionization/recombination Atomic Processes in the AGNs Broad-Line Region

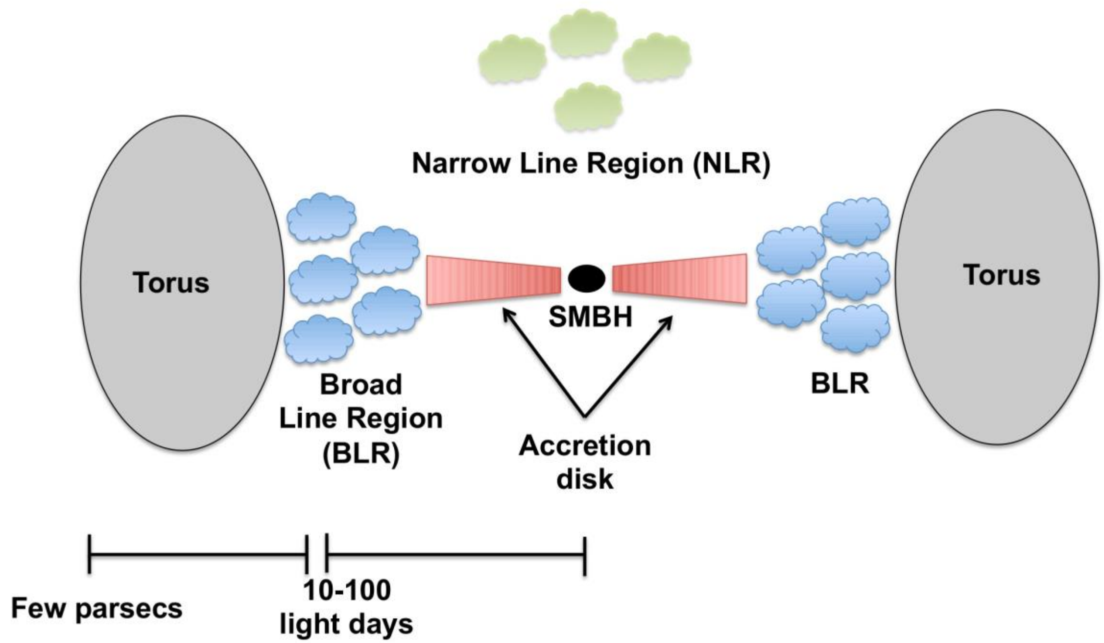

Out main idea

In AGN, especially in the region of the moderately ionized layers of dense parts of the BLR clouds (NeT ~10^{14}cm^{-3}K) plasma conditions are closer to stellar atmospheres than to photoionized nebulae (Osterbrock 1989).

Consequently, it is of interest to investigate the influence of the mentioned processes in dense parts of BLR clouds and to provide the data on the corresponding rate coefficients useful for modelling and investigations of such layers.

Mercè Crosas and Jon C. Weisheit, Hydrogen molecules in quasar broad-line regions, MNRAS, 1993, 262, 359.

we started to check the literature. problems

No rate coefficients for higher n
and
No rate coefficients for second non-associative channel

the uncertainties of the rate coefficients due to hydrogen collisions exist in almost all cases

For the conditions 10^4 - 10^{10} cm^{-3} they concluded that the influence of the associative chemi -ionization processes is negligible in BLR clouds.

However, in very dense weakly ionized regions with > 10^{10} cm^{-3} , these chemi ionization / recombination processes could be important and could change the optical characteristics

Table 2. Collisional reactions.

Reaction	Rate Coefficient (cm^3/s)		Ref
1. $H^+ + e^- \rightarrow H + h\nu$	$K_1 = 1.59 \times 10^{-13} T_4^{-0.5} e^{-\tau_{LL}} + 2.6 \times 10^{-13} T_4^{-0.85}$		1
2. $H + e^- \rightarrow H^- + h\nu$	$K_2 = 2.65 \times 10^{-15} T_4 + 1.22 \times 10^{-15}$		2
3. $H^- + H \rightarrow H_2 + e^-$	$K_3 = 2.7 \times 10^{-9}$		3
4. $H^- + H^+ \rightarrow H + H$	$K_4 = 7.0 \times 10^{-9} T_4^{-0.5}$		4
5. $H^- + H_2^+ \rightarrow H + H + H$; $\rightarrow H_2 + H$	$K_5 = 5.0 \times 10^{-8} T_4^{-0.5}$		4
6. $H^+ + H \rightarrow H_2^+ + h\nu$	$K_6 = 2.9 \times 10^{-16} T_4^{-1.8}$,	$T < 6700K$	5
	$K_6 = 5.8 \times 10^{-16} (T_4/5.6)^{-0.66 \log 10(T_4/5.6)}$,	$T > 6700K$	5
7. $H_2^+ + H \rightarrow H_2 + H^+$	$K_7 = 6.4 \times 10^{-10}$		6
8. $H_2 + H^+ \rightarrow H_2^+ + H$	$K_8 = 2.4 \times 10^{-9} e^{-2.12/T_4}$		7
9. $H_2^+ + e^- \rightarrow H^+ + H + e^-$	$K_9 = 2.0 \times 10^{-8}$		8
10. $H_2 + e^- \rightarrow 2H + e^-$	$K_{10} = 1.1 \times 10^{-8} e^{-10.2/T_4} T_4^{0.35}$		5
11. $H_2 + e^- \rightarrow H^- + H$	$K_{11} = 9.69 \times 10^{-13} e^{-11.323/(\ln 10^4 T_4 - 7.28)}$		5
12. $H+H+H \rightarrow H_2 + H$	$K_{12} = 5.5 \times 10^{-33} T_4^{-1}$		5
13. $H_2 + H \rightarrow H + H + H$	$K_{13} = 6.53 \times 10^{-9} e^{-5.24/T_4}$		5
14. $H_2 + H + H \rightarrow H_2 + H_2$	$K_{13} = K_{10}/8$		5
15. $H_2 + H_2 \rightarrow H_2 + H + H$	$K_{15} = 11.3 \times 10^{-9} e^{-5.33/T_4}$		5
16. $H(n=1) + H^*(n=2) \rightarrow H_2^* \rightarrow H_2 + h\nu$	$K_{16} = 5.0 \times 10^{-14}$		9
17. $H(n=1) + H^*(n=2) \rightarrow H_2^+ + e^-$	$K_{17} = 8.73 \times 10^{-12} T_4^{0.95}$,	$T < 5000K$	10
	$K_{17} = 2.9 \times 10^{-11} T_4^{2.69}$,	$T > 5000K$	10
18. $H(n=1) + H^*(n=3) \rightarrow H_2^+ + e^-$	$K_{18} = 4.42 \times 10^{-11} T_4^{0.95} e^{0.87/T_4}$,	$T < 5000K$	11
	$K_{18} = 1.47 \times 10^{-10} T_4^{2.69} e^{0.87/T_4}$,	$T > 5000K$	11

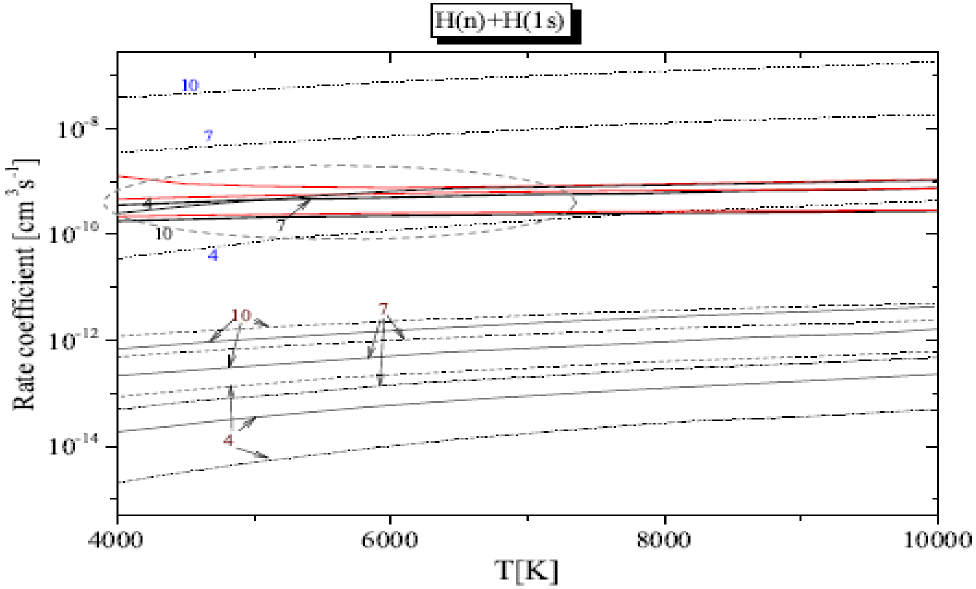

Figure 2. Plot of collisional ionisation H(n) + H($1s$) rate coefficients for selected temperatures and excited states (n=4, 7, 10). The black lines are the data analyzed in Barklem (2007) for non associative channel 4, where A = H. The data from Mihajlov and coworkers based on the same mechanism as here are plotted as thick full lines. The numerical data from Soon (1992) are plotted as normal full lines and the dot-dashed line (see Barklem (2007) for detailed explanation). The data from Soon's analytic expressions are plotted as dashed lines, and the data from Drawin (1968, 1969) are plotted as dotted lines. The red lines are summary rate coefficients for associative (3) and non-associative (4) channels (this work). The rate coefficients for whole range of n and T i.e. $2 \leq n \leq 20$, and $4000\ K \leq T \leq 20000\ K$ can be found in the Tables 2-7 in the online version of the article.

the uncertainties of the rate coefficients due to hydrogen collision

Cross sections
for channel a) and b)

$$\sigma_{\mathrm{ci}}^{(a,b)}(n, E) = 2\pi \int_0^{\rho_{\max}^{(a,b)}(E)} P_{\mathrm{ci}}^{(a,b)}(n, \rho, E)\rho d\rho,$$

Rate coefficient for channel a) and b)

$$K_{\mathrm{ci}}^{(a,b)}(n, T) = \int_{E_{\min}^{(a,b)}(n)}^{E_{\max}} v\sigma_{\mathrm{ci}}^{(a,b)}(n, E) f(v; T) dv,$$

Total rate coefficient

$$K_{\mathrm{ci}}(n, T) = K_{\mathrm{ci}}^{(a)}(n, T) + K_{\mathrm{ci}}^{(b)}(n, T),$$

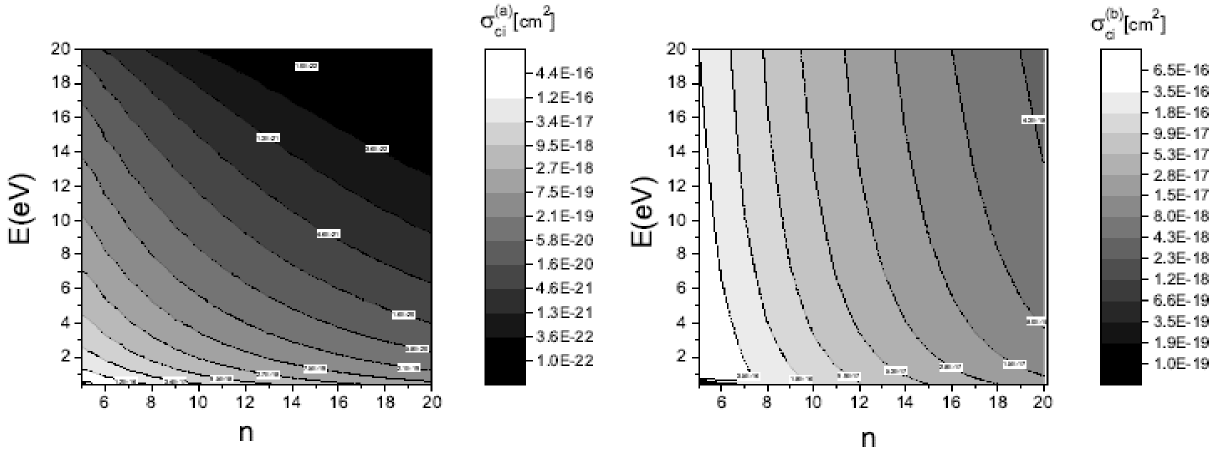

Figure 1. a) b)
a) The surface plot of the partial cross section $\sigma_{ci}^{(a)}(n, E)$ Eq.(12) which characterizes the efficiency of the chemi-ionization processes (3) i.e. associative ionization channel. b) The surface plot of the partial cross sections $\sigma_{ci}^{(b)}(n, E)$ Eq. (12) which characterizes the efficiency of the chemi-ionization processes (4) i.e. non-associative ionization channel.

Table 1. Calculated Values of Coefficient K_{ci}[cm^3/s] as a Function of n and T. A portion is shown here for guidance regarding its form and content.

T/n	10	11	12	13	14	15	16	17	18	19	20
4000	2.17E-10	1.68E-10	1.31E-10	1.03E-10	8.19E-11	6.57E-11	5.32E-11	4.35E-11	3.58E-11	2.97E-11	2.49E-11
5000	2.36E-10	1.81E-10	1.40E-10	1.09E-10	8.62E-11	6.88E-11	5.55E-11	4.52E-11	3.72E-11	3.08E-11	2.57E-11
6000	2.51E-10	1.90E-10	1.46E-10	1.14E-10	8.94E-11	7.12E-11	5.73E-11	4.65E-11	3.82E-11	3.16E-11	2.63E-11
7000	2.62E-10	1.98E-10	1.51E-10	1.17E-10	9.20E-11	7.30E-11	5.86E-11	4.76E-11	3.89E-11	3.22E-11	2.68E-11
8000	2.71E-10	2.04E-10	1.55E-10	1.20E-10	9.40E-11	7.45E-11	5.97E-11	4.84E-11	3.96E-11	3.26E-11	2.72E-11
9000	2.79E-10	2.09E-10	1.59E-10	1.22E-10	9.57E-11	7.57E-11	6.06E-11	4.90E-11	4.01E-11	3.30E-11	2.75E-11
10000	2.85E-10	2.13E-10	1.62E-10	1.24E-10	9.71E-11	7.67E-11	6.14E-11	4.96E-11	4.05E-11	3.34E-11	2.77E-11
11000	2.91E-10	2.17E-10	1.64E-10	1.26E-10	9.83E-11	7.76E-11	6.20E-11	5.01E-11	4.09E-11	3.36E-11	2.79E-11
12000	2.96E-10	2.20E-10	1.66E-10	1.28E-10	9.93E-11	7.83E-11	6.25E-11	5.05E-11	4.12E-11	3.39E-11	2.81E-11
13000	3.00E-10	2.23E-10	1.68E-10	1.29E-10	1.00E-10	7.90E-11	6.30E-11	5.09E-11	4.14E-11	3.41E-11	2.83E-11
14000	3.04E-10	2.25E-10	1.70E-10	1.30E-10	1.01E-10	7.96E-11	6.35E-11	5.12E-11	4.17E-11	3.43E-11	2.84E-11
15000	3.08E-10	2.28E-10	1.71E-10	1.31E-10	1.02E-10	8.01E-11	6.38E-11	5.15E-11	4.19E-11	3.44E-11	2.86E-11
16000	3.11E-10	2.30E-10	1.73E-10	1.32E-10	1.02E-10	8.06E-11	6.42E-11	5.17E-11	4.21E-11	3.46E-11	2.87E-11
17000	3.14E-10	2.31E-10	1.74E-10	1.33E-10	1.03E-10	8.10E-11	6.45E-11	5.19E-11	4.23E-11	3.47E-11	2.88E-11
18000	3.16E-10	2.33E-10	1.75E-10	1.34E-10	1.04E-10	8.14E-11	6.48E-11	5.21E-11	4.24E-11	3.48E-11	2.89E-11
19000	3.19E-10	2.35E-10	1.76E-10	1.34E-10	1.04E-10	8.17E-11	6.50E-11	5.23E-11	4.26E-11	3.50E-11	2.90E-11
20000	3.21E-10	2.36E-10	1.77E-10	1.35E-10	1.04E-10	8.20E-11	6.52E-11	5.25E-11	4.27E-11	3.51E-11	2.90E-11

chemi-ionization processes:

$$A^*(n) + A \Rightarrow A_2^+ + e$$

$$A^*(n) + A \Rightarrow A + A^+ + e$$

Invers chemi-recombination processes:

$$A_2^+ + e \Rightarrow A^*(n) + A$$

$$A + A^+ + e \Rightarrow A^*(n) + A$$

We compare with the corresponding electron-atom collision processes

$$A^*(n) + e \Rightarrow A^+ + 2e,$$

$$A^+ + 2e \Rightarrow A^*(n) + e,$$

$$A^+ + e \Rightarrow A^*(n) + \varepsilon_\lambda,$$

Comparison of Fluxes of the Considered Processes

$$I_{\mathrm{ci}}(n, T) = K_{\mathrm{ci}}(n, T) \cdot N_n N_1,$$
$$I_{\mathrm{cr}}(n, T) = K_{\mathrm{cr}}(n, T) \cdot N_1 N_i N_e,$$

$$I_{i;\mathrm{ea}}(n, T) = K_{\mathrm{ea}}(n, T) \cdot N_n N_e,$$
$$I_{r;\mathrm{eei}}(n, T) = K_{\mathrm{eei}}(n, T) \cdot N_i N_e N_e,$$
$$I_{r;\mathrm{ph}}(n, T) = K_{\mathrm{ph}}(n, T) \cdot N_i N_e,$$

$$F_i(n, T) = \frac{I_{\mathrm{ci}}(n, T)}{I_{i;\mathrm{ea}}(n, T)} = \frac{K_{\mathrm{ci}}(n, T)}{K_{\mathrm{ea}}(n, T)} \cdot N_1 N_e,$$

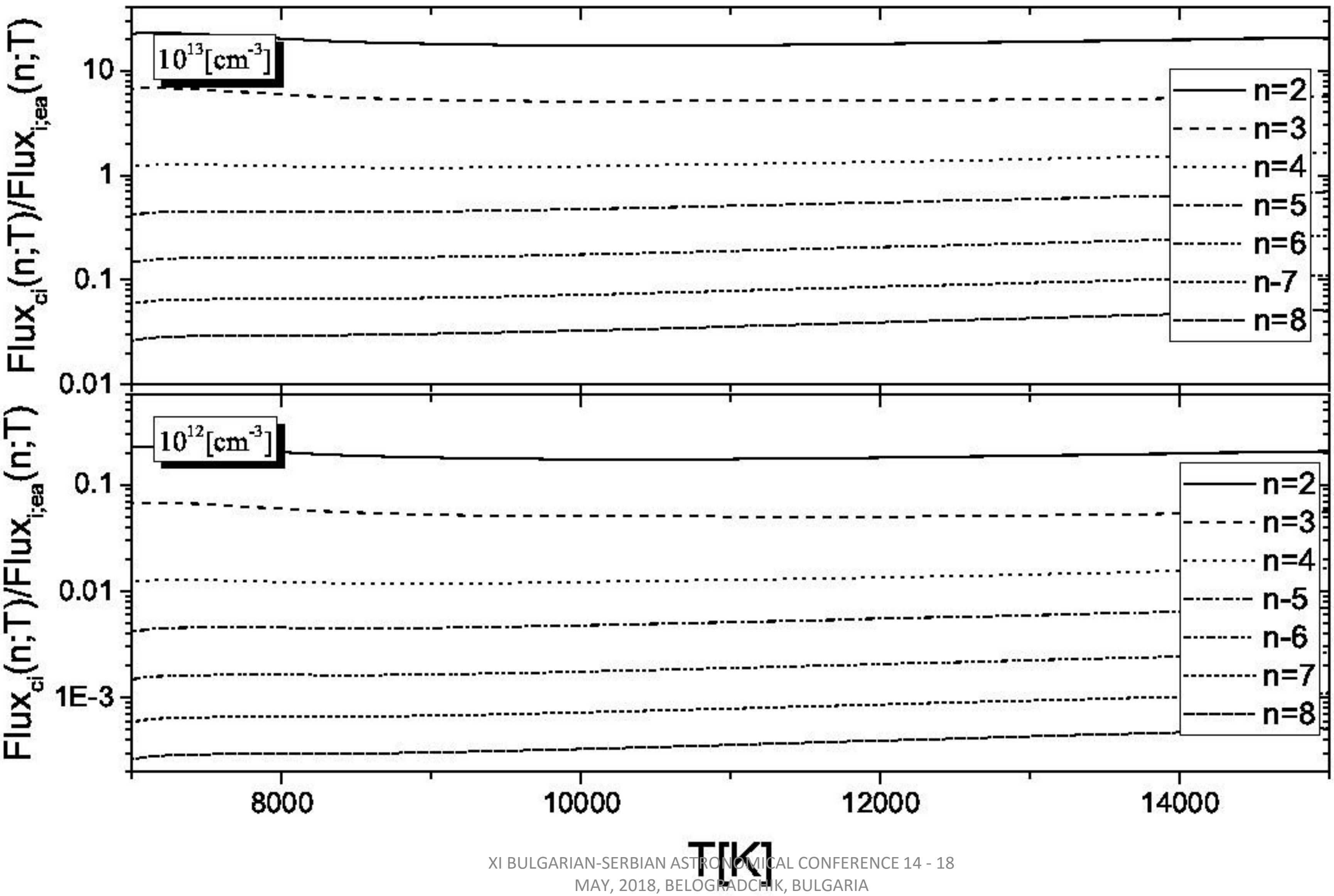

10^{13}[cm^{-3}]
10^{12}[cm^{-3}]
n=2
n=3
n=4
n=5
n=6
n-7
n=8
n=2
n=3
n=4
n-5
n-6
n=7
n=8
Flux$_{ci}$(n;T)/Flux$_{i,ea}$(n;T)
Flux$_{ci}$(n;T)/Flux$_{i,ea}$(n;T)
10
1
0.1
0.01
0.1
0.01
1E-3
8000
10000
12000
14000
T[K]

DISCUSSION AND CONCLUSION

We can see as well that even around the value of N1 = 10^{12} cm^{-3} the inclusion of the considered here chemi-ionization/recombination processes could improve the modelling and analysis of such regions not only in photospheres of Sun and solar like stars but also in clouds in AGN BLR and NRL.

Additionally, the Figure 3 demonstrates as well the high sensitivity of the influence of these processes to the relatively small changes of N1 which can be of interest for the determination of limiting N1 densities in clouds in AGN BLR and NRL.

submitted in MNRAS

perspectives

Our plan is to present the results obtained during this investigation in MolD database which can be accessed directly through http://servo.aob.rs as a web service (Marinković et al., 2017; Srećković, Ignjatović, Jevremović, Vujčić, & Dimitrijević, 2017).

Website User Interface

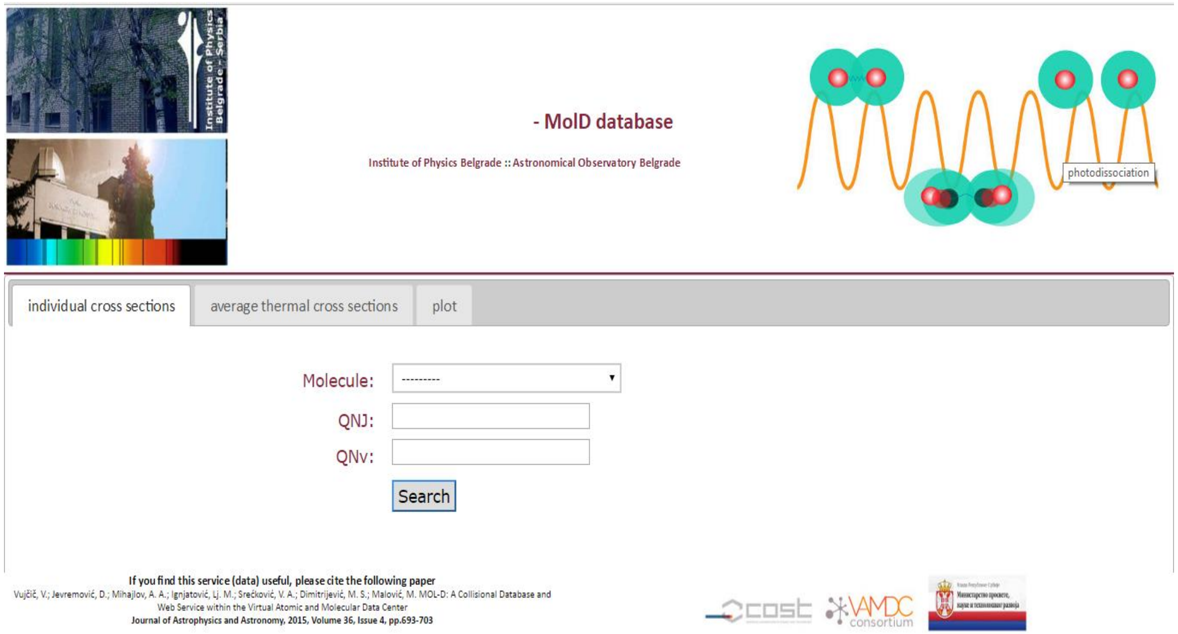

Or

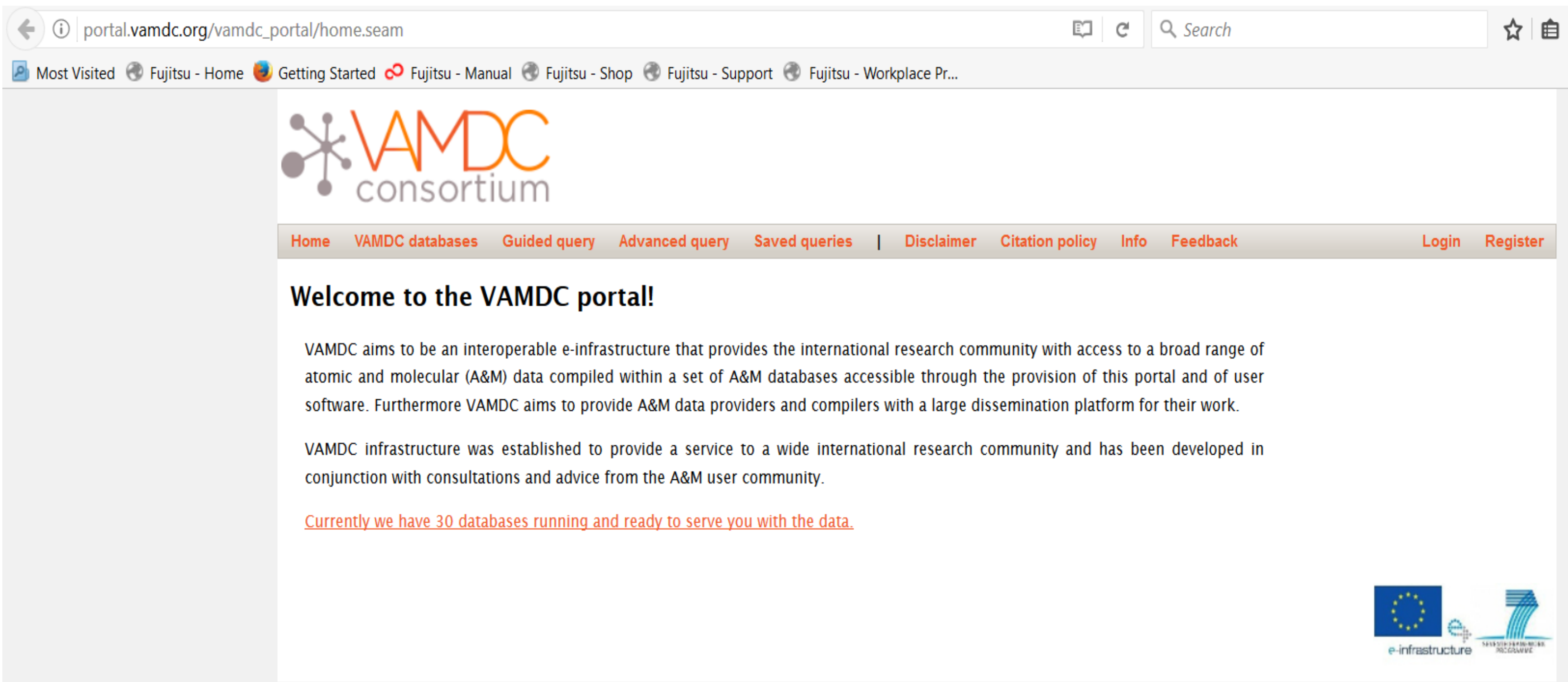
portal.vamdc.org/vamdc_portal/home.seam
Search
Most Visited
Fujitsu - Home
Getting Started
Fujitsu - Manual
Fujitsu - Shop
Fujitsu - Support
Fujitsu - Workplace Pr...
VAMDC consortium
Home
VAMDC databases
Guided query
Advanced query
Saved queries
Disclaimer
Citation policy
Info
Feedback
Login
Register
Welcome to the VAMDC portal!
VAMDC aims to be an interoperable e-infrastructure that provides the international research community with access to a broad range of atomic and molecular (A&M) data compiled within a set of A&M databases accessible through the provision of this portal and of user software. Furthermore VAMDC aims to provide A&M data providers and compilers with a large dissemination platform for their work.
VAMDC infrastructure was established to provide a service to a wide international research community and has been developed in conjunction with consultations and advice from the A&M user community.
Currently we have 30 databases running and ready to serve you with the data.
e-infrastructure

Map of databases (on all continents)

VAMDC: technical organisation

- A set of standards
  Data exchange protocols, data description
  Standard vocabulary for all exchanges, including for registration of ressources
- A set of software
- Documentation and online support system

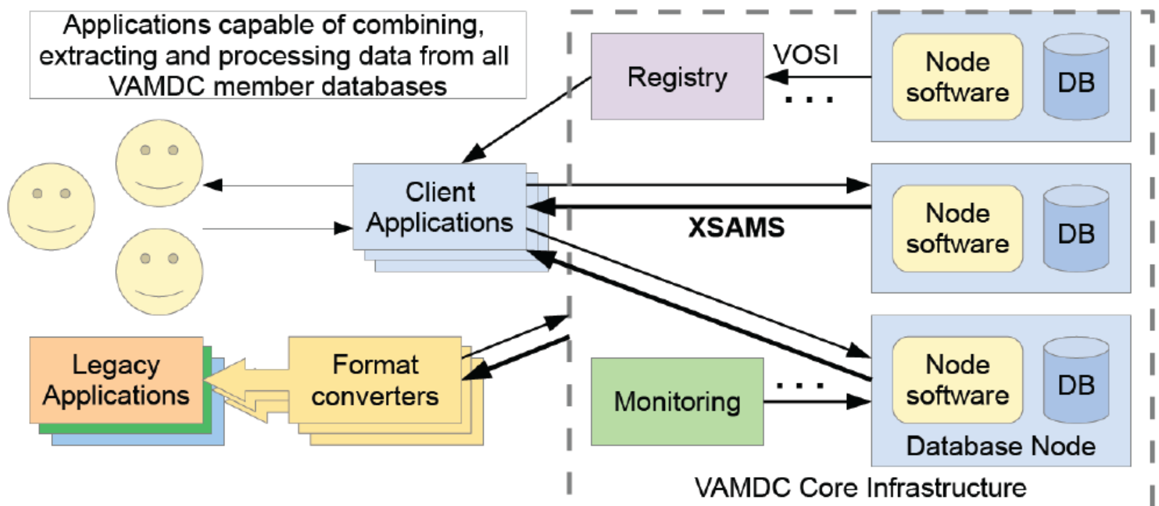

Molecule: Hydrogen molecular ion: H2+

QNJ: 3

QNv: 2

Search


```
-<XSAMSData xmlns="http://vamdc.org/xml/xsams/1.0" xmlns:xsi="http://www.w3.org/2001/XMLSchema-instance"
xmlns:cml="http://www.xml-cml.org/schema" xsi:schemaLocation="http://vamdc.org/xml/xsams/1.0 http://vamdc.org/xml/xsams
/1.0">
 +<Sources> </Sources>
 -<Species>
  -<Molecules>
   -<Molecule speciesID="XmolD-2">
    -<MolecularChemicalSpecies>
     +<OrdinaryStructuralFormula> </OrdinaryStructuralFormula>
     -<StoichiometricFormula>H2+</StoichiometricFormula>
     +<ChemicalName> </ChemicalName>
     -<InChI>1S/H2/h1H/q+1</InChI>
     -<InChIKey>ZZIJOQHRUPVPQC-UHFFFAOYSA-N</InChIKey>
     <VAMDCSpeciesID />
     -<StableMolecularProperties> </StableMolecularProperties>
    </MolecularChemicalSpecies>
    -<MolecularState auxillary="false" stateID="SmolD-895">
     -<Description>r: 3, v: 2</Description>
     -<MolecularStateCharacterisation>
      -<StateEnergy energyOrigin="SmolD-1258">
       -<Value units="au">-.765732110396E-01</Value>
      </StateEnergy>
     </MolecularStateCharacterisation>
     +<Case xsi:type="case:Case" caseID="dcs" xmlns:case="http://vamdc.org/xml/xsams/1.0/cases/dcs"> </Case>
    </MolecularState>
    +<MolecularState auxillary="true" stateID="SmolD-1258"> </MolecularState>
   </Molecule>
  </Molecules>
 </Species>
 +<Processes> </Processes>
 -<Processes>
  -<Radiative>
   -<AbsorptionCrossSection id="PmolD-CS895">
    -<SourceRef>BmolD-1</SourceRef>
    -<SourceRef>BmolD-6</SourceRef>
    +<X units="nm"> </X>
    -<X units="nm">
     -<DataList count="226">
      50 51 52 53 54 55 56 57 58 59 60 61 62 63 64 65 66 67 68 69 70 71 72 73 74 75 76 77 78 79 80 81 82 83 84 85 86 87 88 89 90
      91 92 93 94 95 96 97 98 99 100 101 102 103 104 105 106 107 108 109 110 111 112 113 114 115 116 117 118 119 120 121 122 123
      124 125 126 127 128 129 130 131 132 133 134 135 136 137 138 139 140 141 142 143 144 145 146 147 148 149 150 151 152 153 154
      155 156 157 158 159 160 161 162 163 164 165 166 167 168 169 170 171 172 173 174 175 176 177 178 179 180 181 182 183 184 185
      186 187 188 189 190 191 192 193 194 195 196 197 198 199 200 205 210 215 220 225 230 235 240 245 250 255 260 265 270 275 280
      285 290 295 300 305 310 315 320 325 330 335 340 345 350 355 360 365 370 375 380 385 390 395 400 405 410 415 420 425 430 435
      440 445 450 455 460 465 470 475 480 485 490 495 500 600 700 800 900 1000 1100 1200 1300 1400 1500 1600 1700 1800 1900 2000
     </DataList>
    </X>
    -<Y units="cm2">
     -<DataList count="226">
      0.228892E-21 0.433293E-21 0.811722E-21 0.145515E-20 0.250921E-20 0.424328E-20 0.702508E-20 0.112831E-19 0.175930E-19
      0.267734E-19 0.398270E-19 0.578434E-19 0.820590E-19 0.113982E-18 0.155347E-18 0.207896E-18 0.273231E-18 0.352807E-18
      0.447915E-18 0.559472E-18 0.687723E-18 0.832109E-18 0.991387E-18 0.116384E-17 0.134729E-17 0.153892E-17 0.173497E-17
      0.193076E-17 0.212088E-17 0.229964E-17 0.246148E-17 0.260119E-17 0.271398E-17 0.279557E-17 0.284233E-17 0.285151E-17
      0.282155E-17 0.275226E-17 0.264486E-17 0.250194E-17 0.232728E-17 0.212567E-17 0.190275E-17 0.166491E-17 0.141913E-17
      0.117279E-17 0.933458E-18 0.708595E-18 0.505259E-18 0.329844E-18 0.187854E-18 0.837518E-19 0.208600E-19 0.130658E-20
      0.260073E-19 0.946690E-19 0.205816E-18 0.356843E-18 0.544097E-18 0.762994E-18 0.100817E-17 0.127366E-17 0.155309E-17
      0.183984E-17 0.212729E-17 0.240895E-17 0.267861E-17 0.293048E-17 0.315932E-17 0.336049E-17 0.353007E-17 0.366488E-17
      0.376256E-17 0.382159E-17 0.384131E-17 0.382188E-17 0.376428E-17 0.367026E-17 0.354228E-17 0.338340E-17 0.319721E-17
      0.298774E-17 0.275932E-17 0.251652E-17 0.226404E-17 0.200661E-17 0.174890E-17 0.149548E-17 0.125072E-17 0.101873E-17
      0.803338E-18 0.608032E-18 0.435914E-18 0.289686E-18 0.171621E-18 0.835568E-19 0.268815E-19 0.253852E-20 0.110319E-19
      0.524408E-19 0.126439E-18 0.232318E-18 0.369023E-18 0.535175E-18 0.729119E-18 0.948951E-18 0.119256E-17 0.145768E-17
      0.174189E-17 0.204269E-17 0.235751E-17 0.268376E-17 0.301885E-17 0.336019E-17 0.370528E-17 0.405165E-17 0.439694E-17
      0.473890E-17 0.507538E-17 0.540439E-17 0.572404E-17 0.603263E-17 0.632858E-17 0.661050E-17 0.687713E-17 0.712740E-17
      0.736037E-17 0.757530E-17 0.777158E-17 0.794874E-17 0.810648E-17 0.824465E-17 0.836318E-17 0.846219E-17 0.854187E-17
      0.860253E-17 0.864457E-17 0.866849E-17 0.867486E-17 0.866431E-17 0.863755E-17 0.859530E-17 0.853837E-17 0.846755E-17
```


Sample output from MolD. Data set, represented in XSAMS (XML Schema for Atoms, Molecules and Solids) format.

THANK YOU FOR ATTENTION